



# Impact of product family complexity on process performance in electronic component assembly

Stefano Puttero<sup>1</sup> · Elisa Verna<sup>1</sup> · Gianfranco Genta<sup>1</sup> · Maurizio Galetto<sup>1</sup>

Received: 12 December 2023 / Accepted: 28 March 2024 / Published online: 6 April 2024  
© The Author(s) 2024

## Abstract

With the advent of Industry 4.0 and the impending shift towards Industry 5.0, the integration of human–robot collaboration (HRC) into production systems has become increasingly widespread. This paradigm shift leverages collaborative robots, or cobots, to mitigate physical and mental strain on human workers, thereby increasing productivity and improving overall quality performance. This paper investigates the interplay of productivity and quality factors with assembly complexity in both manual and collaborative assembly systems. The focus is placed on a product family of electronic boards, with varying levels of assembly complexity, to provide a comprehensive comparison between manual assembly and two different collaborative assembly scenarios. Key performance metrics such as assembly time and total defects are evaluated. This case study, rooted in the electronics industry, seeks to provide a valuable perspective on how assembly complexity influences productivity and quality in product family assembly systems. The results of this study aim to contribute to the growing body of knowledge on the implementation of HRC in manufacturing, facilitate informed decision-making and encourage further advances in this rapidly evolving field.

**Keywords** Assembly complexity · Product family · Process performance · Assembly system · Electronic board · Human–robot collaboration (HRC)

## 1 Introduction

In recent years, the field of robotics has undergone a radical transformation with the emergence of human–robot collaboration (HRC). Collaborative robots (also known as cobots) have the ability to work alongside human operators without the need for fences or barriers, thus performing tasks that complement human skills and reduce physical effort [1, 2]. This collaboration allows the effective use of human dexterity, adaptability and problem-solving skills, combined with the precision, speed and repeatability of robots [3].

In the manufacturing sector, HRC has revolutionised the assembly process by combining the unique capabilities of humans and robots. Assembly processes, which are a critical task of manufacturing operations, have traditionally relied on human workers to perform complex tasks. However,

limitations inherent in human capabilities, such as physical fatigue, cognitive limitations and repetitive task stress, have prompted the search for alternative solutions to optimise the assembly workflow [4]. Coupled with the continued refinement of robotics and artificial intelligence, HRC has opened up new ways to improve the efficiency, productivity and quality of assembly operations [3].

Another key aspect driving the adoption of HRCs in assembly processes is mass customisation within the framework of Industry 4.0 [5]. In today's market, customers are increasingly demanding customised products. This trend shifts the production paradigm from mass production to mass customization, in which companies must be able to meet different customer demands with a flexible production system [6]. In this intricate framework demanding flexibility and precision, mass customisation strategies have been found to greatly benefit from product family approaches, which cater effectively to the burgeoning customer demands. The principle underpinning this approach involves the creation of a product platform composed of compatible modular components. These modules can be configured to generate a multitude of diverse products, each designed for different purposes yet sharing certain common

✉ Elisa Verna  
elisa.verna@polito.it

<sup>1</sup> Department of Management and Production Engineering,  
Politecnico Di Torino, Corso Duca Degli Abruzzi 24,  
10129 Turin, Italy

characteristics [7]. However, such an approach leads to greater complexity in the production system and in the products themselves. In this new manufacturing paradigm, where flexibility and precision are required, the symbiosis between human and robot offers a promising solution to meet these challenges [8].

This paper aims to explore and analyse the various aspects of the use of HRC in assembly processes, making a comparison with purely manual assembly. It examines several problems in today's manufacturing, including the benefits of human–robot collaboration, the challenges of system integration and the impact on productivity and assembly quality of such integration. The aim is to investigate whether the assembly complexity and the nature of the assembly process have an impact on the performance of the process itself. In detail, the following Research Questions (RQs) are addressed:

- *RQ1*: Does the productivity and quality of the assembly process depend on the assembly complexity and the product characteristics within a product family?
- *RQ2*: Are there statistically significant differences in process productivity and quality between different assembly systems (a manual system, a cobot-assisted system and a cobot system with camera assistance) when applied to various products within a product family?

To answer these questions, three different experimental campaigns for the assembly of electronic boards were carried out. The first experiment consisted of a fully manual assembly of electronic boards, while the other two experiments involved a collaborative robot to support the operator during the assembly. The study of electronic board assembly is motivated by its widespread use in HRC industry applications [9]. Furthermore, electronic boards allow different products to be assembled from the same components, thus emulating the growing demand for customised products in today's market.

The remainder of the paper is organized into six sections. Section 2 introduces the main application of HRC in assembly processes. Section 3 summarizes the main definitions of assembly complexity and defines the methodology proposed to assess the assembly complexity of electronic boards. Section 4 illustrates a case study concerning the practical application of the proposed methodology in manual and collaborative assembly processes. Section 5 presents the research methods, while Section 6 discusses the experimental results. Finally, Section 7 concludes the paper.

## 2 HRC and assembly processes

The manufacturing industry is witnessing a notable transition in automation and robotics, moving away from traditional mass production models and embracing the era

of mass customization. This shift has prompted extensive research and development efforts to address the challenges posed by unstructured industrial environments [6, 10]. As a result, traditional manufacturing approaches are being reimagined to ensure seamless integration between human workers and intelligent machines like cobots. This necessitates the development of novel methodologies and technologies that facilitate efficient collaboration, enhance productivity and enable swift adaptation to changing production demands.

The shift from mass production to mass customisation mainly influenced the assembly and disassembly processes [11]. This can be attributed in part to the fact that the assembly process, unlike an automated process, allows for customisation of products. Particularly, an assembly process can be defined as a series of sequential activities involving the joining of geometrically defined parts, components and software to create functional products [12]. This process has distinct characteristics compared to traditional manufacturing, such as a large number of parts, numerous variations, frequent production interruptions and shorter cycle times. Accordingly, given the human cognitive ability and flexibility to adapt to different situations, assembly systems have traditionally relied on human labour and have remained separate from traditional automation [13].

Nevertheless, on-going developments in automation and collaborative robotics, as well as the incorporation of artificial intelligence and machine learning, present significant opportunities to improve assembly processes. The goal is to develop intelligent systems that can easily interact with human operators and understand, adapt and respond to changing assembly needs. The integration between humans and robots in assembly processes can lead to three main advantages [13, 14]:

- **Increased efficiency:** Collaborative robots are excellent at performing time-consuming and repetitive tasks, freeing human workers from tedious tasks. Cobots greatly improve assembly line productivity by automating these processes, reducing cycle times and increasing throughput.
- **Improved quality:** The accuracy and consistency of collaborative robots help assembly operations produce higher-quality products. The possibility of errors and rework is reduced by cobots' ability to maintain high levels of precision during component insertion, tightening and other critical assembly operations.
- **Flexibility and safety:** The collaborative configuration allows human dexterity and adaptability to be combined with the precision and repeatability of cobots. This collaboration is made possible by the use of advanced sensors and algorithms to detect and respond to human presence, enabling cobots to work safely alongside human

operators. This feature eliminates the need for physical barriers, making cobots a more flexible alternative for assembly operations.

This collaborative configuration is commonly observed in manufacturing environments. One example is the automotive sector [15, 16], where cobots are used to assist human operators with tasks such as tightening bolts, installing seals, fitting bearings and lifting heavy loads. Another important application is in the electronics industry (which will be discussed in this paper), where cobots assist operators in assembling electronic circuit boards [17]. In both industrial sectors, the use of cobots has led to improvements in efficiency, quality and safety, while reducing the risk of repetitive strain injuries for human operators.

However, the HRC working environment is dynamic and complex. These systems must be able to grow and adapt to different configurations as they are designed to deliver a wide range of products. In this context, intelligent job allocation becomes crucial, requiring complex design to meet the requirements of intelligent production systems. Innovative approaches to human–machine collaboration are required due to the dynamic nature of product requirements and the ever-changing socio-economic environment. Industry and researchers are being forced to explore new approaches to meet these changing needs and effectively address the complexities of collaborative assembly in the age of smart manufacturing [4].

### 3 Assembly complexity of electronic boards

Recent research has shown that assembly complexity plays a fundamental role in the performance of operators and assembly processes [18, 19]. Assembly complexity has been shown to affect key performance indicators such as assembly time, quality defects and production costs. The implications of these findings are far-reaching. Complex tasks or processes tend to have longer assembly times because they require additional steps or complex procedures and increase the likelihood of quality defects [20]. In addition, increased assembly complexity can lead to higher production costs due to the need for specialised resources, advanced equipment or additional labour [21, 22]. It is therefore essential to recognise and manage assembly complexity effectively to optimise operator and production process performance.

In order to analyse how assembly complexity affects the productivity and quality of a process, the assembly of ARDUINO electronic boards was considered in this study. These boards allow the utilization of similar components for assembling high personalized products characterized by varying degrees of assembly complexity, all while ensuring real-time monitoring of proper assembly and functionality.

### 3.1 Assembly complexity modelling

As stated above, modelling the assembly complexity is crucial for studying the productivity and quality of the process. Several articles and reviews already exist addressing methods to assess and manage assembly complexity in manufacturing [21, 23–25]. In this paper, the assembly complexity model based on Huckel’s molecular theory is used to assess the assembly complexity of electronic boards [26]. By dividing assembly complexity into the definition of different factors, Hückel’s theory simplifies the modelling of assembly complexity. This model can determine the assembly complexity of any network-based engineering system, taking into account three key factors: the complexity of the individual components ( $C_1$ ); the pairwise interaction between the connected components ( $C_2$ ); the overall topology of the system ( $C_3$ ). By combining these three factors, it is possible to quantify the overall assembly complexity (denoted by  $C$ ) with the following expression:

$$C = C_1 + C_2 \cdot C_3 \quad (1)$$

$C_1$  refers to the intricacy of managing and interacting with each individual component in isolated conditions. It measures the complexity associated with handling the product component.  $C_1$  can be calculated as:

$$C_1 = \sum_{m=1}^N h_m \quad (2)$$

where  $N$  is the total number of product components, and  $h_m$  is the handling complexity of component  $m$ . The handling complexity  $h_m$  can be calculated using the Lucas method [27], a method rooted in the principles of design for assembly (DFA). Using a point scale, the Lucas method provides a relative measure of assembly difficulty that results in a normalized handling complexity index. This index considers a range of factors such as the size, weight, handling difficulty and orientation (alpha and beta symmetry) of each individual component (see Table 1).

The Lucas method assigns a distinct handling complexity index to each component, as it will be illustrated in Section. 3.2 for the electronic boards. The higher the value of  $h_m$ , the more challenging it becomes to handle and position the component on the board. These values are determined as:

$$h_m = \frac{h_m^A + \sum_{i=1}^{N_B} h_m^B + h_m^C + h_m^D}{h_{max}} \quad (3)$$

where  $h_m^{i \in \{A,B,C,D\}}$  is the handling difficulty of  $i^{th}$  attribute,  $N_B$  is the number of applicable handling difficulties related to attribute  $B$ , and  $h_{max}$  is the theoretical maximum value for the handling index (i.e., 6.9, according to Table 1).

**Table 1** Difficulty of component handling attributes. Adapted from Chan and Salustri [27]

Attribute <i>i</i>	Description	<i>h<sub>m</sub></i>
A. Size and weight (one of the following)	Very small—requires handling aids	1.5
	Easy—requires one hand only	1
	Large and/or heavy—requires more than one hand or aid	1.5
	Large and/or heavy—requires hoist or more than one person	2
B. Handling difficulty (all that apply)	Delicate	0.4
	Flexible	0.6
	Sticky	0.5
	Tangible	0.8
	Severely nest	0.7
	Sharp/abrasive	0.3
	Untouchable	0.5
	Gripping problem/slippery	0.2
	Automatic handling—no difficulty	0
	Symmetrical—no orientation required	0
C. Alpha symmetry (one of the following)	Easy to orient—end to end	0.1
	Difficult to orient—end to end	0.5
	Rotational orientation is not required	0
D. Beta symmetry (one of the following)	Easy to orient—end to end	0.2
	Difficult to orient—end to end	0.4

$C_2$  is the complexity of connections and liaisons between parts. According to Eq. (4),  $C_2$  is calculated as the sum of the complexities of the pairwise connections present in the product structure:

$$C_2 = \sum_{m=1}^{N-1} \sum_{n=m+1}^N l_{mn} \cdot i_{mn} \quad (4)$$

where  $l_{mn}$  is the complexity in achieving a connection between components  $m$  and  $n$ , and  $i_{mn}$  is the  $(m, n)^{\text{th}}$  entry of the binary adjacency matrix ( $\mathbf{AM}$ ) of the product. The complexity  $l_{mn}$  is calculated with the Lucas method [27], by using the difficulty of connection attributes in Table 2.

The Lucas method provides a standardised assembly index that takes into account various physical attributes that contribute to assembly complexity. These attributes include factors such as component positioning and fastening, assembly direction, visibility, alignment and resistance to insertion. The index penalises those physical attributes that directly affect the difficulty of the assembly process. Accordingly,  $l_{mn}$  is obtained as follows:

$$l_{mn} = \frac{c_d^E + c_d^F + c_d^G + c_d^H + c_d^I + c_d^J + c_d^K}{c_{\max}} \quad (5)$$

where  $c_d^{j \in \{E, F, G, H, I, J, K\}}$  is the handling difficulty of  $j^{\text{th}}$  attribute, and  $c_{\max}$  is the theoretical maximum value for the connection index (i.e., 13.1, according to Table 2).

In Eq. (4),  $i_{mn}$  is defined by using the symmetric binary adjacent matrix ( $\mathbf{AM}$ ) of the product. Each entry in the  $\mathbf{AM}$

matrix indicates the presence of an assembly connection between two components. Accordingly,  $i_{mn}$  can assume two different values:

$$i_{mn} = \begin{cases} 1, & \text{if there is a connection between } m \text{ and } n \\ 0, & \text{otherwise} \end{cases} \quad (6)$$

Finally, topological complexity  $C_3$ , i.e., the complexity of product architectural pattern, is defined as:

$$C_3 = \frac{E_{AM}}{N} = \frac{\sum_{q=1}^N \delta_q}{N} \quad (7)$$

where  $E_{AM}$  is the matrix energy of  $\mathbf{AM}$ , i.e. the sum of the singular values  $\delta_q$  of  $\mathbf{AM}$  [28]. Since the adjacency matrix  $\mathbf{AM}$  is a symmetric matrix of size  $N \times N$  with all diagonal elements equal to zero, the singular values correspond to the absolute eigenvalues of the adjacency matrix. The  $E_{AM}$  value increases when the system moves from centralised to more distributed architectures.

### 3.2 Complexity of electronic boards assembly

An experimental campaign was conducted to assemble a product family composed of six different variants of electronic boards using the ARDUINO UNO starter kit (ARDUINO®). Fig. 1 shows the six electronic boards assembled during the experiments. The aim of the experiment was to study the complexity of assembly and how it affects assembly time and the quality of the assembled

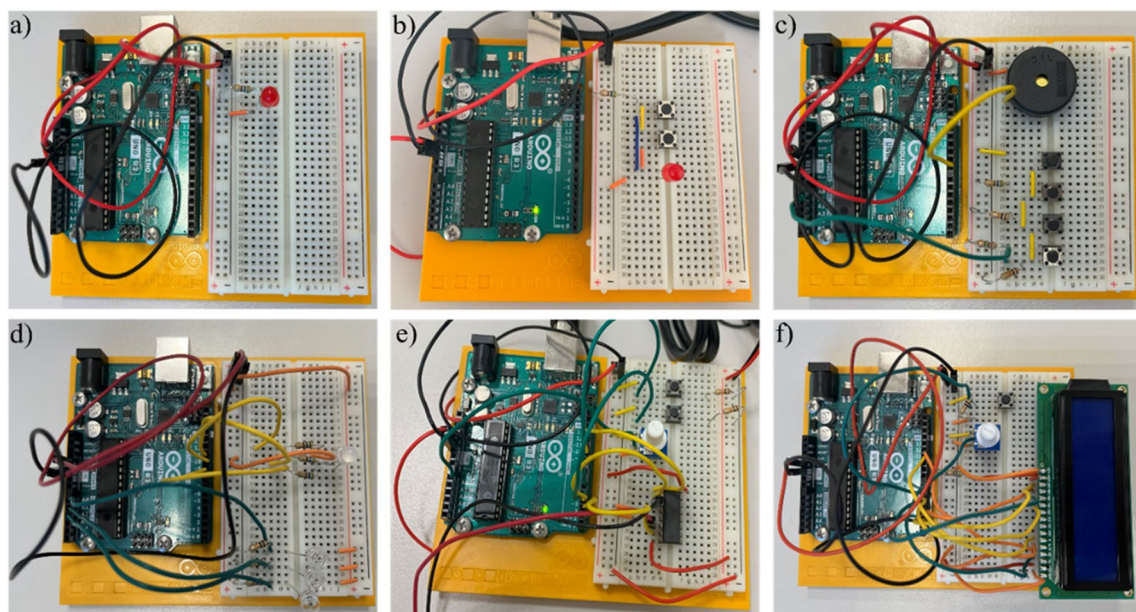


**Table 2** Difficulty of component connection attributes. Adapted from Chan and Salustri [27]

Attribute $j$	Description	$c_d$
E. Component placing (one of the following)	Self-holding	1
	Holding down required	2
F. Component fastening (one of the following)	Self-securing	1.3
	Screwing	4
	Riveting	4
	Bending	4
	Mechanical deformation	4
	Soldering or welding	6
	Adhesive	5
G. Direction (one of the following)	Straight line from above	0
	Straight line not from above	0.1
	Not straight line and/or bending is required	1.6
H. Insertion (one of the following)	Single	0
	Multiple	0.7
	Simultaneous multiple insertions	1.2
I. Restricted vision (one of the following)	Visible	0
	Not visible	1
J. Difficult to align (one of the following)	No	0
	Yes	0.7
K. Resistance to insertion (one of the following)	No	0
	Yes	0.6

products. In particular, using electronic boards as an assembly product has two main advantages: firstly, they allow a high degree of customization of products using the same starting components; secondly, they are widely used in HRC [17]. As shown in Fig. 1, the ARDUINO boards consist of

three main parts: (i) the components that are assembled (e.g. wires, pushbuttons, resistors), (ii) the microcontroller that enables the circuit's functionality and (iii) the breadboard where the circuits are built. This particular type of breadboard has rows and columns of holes that conduct electricity,

**Fig. 1** Example of the six assembled electronic boards **a** product 1 (P1); **b** product 2 (P2); **c** product 3 (P3); **d** product 4 (P4); **e** product 5 (P5); **f** product 6 (P6)

**Table 3** Characteristics of the six assembled electronic boards (P1–P6)

Component	P1	P2	P3	P4	P5	P6
Breadboard	1	1	1	1	1	1
Long wires	-	1	2	8	9	13
Short wires	1	3	5	3	6	4
Resistors	1	1	4	6	2	2
Pushbuttons	-	2	4	-	2	1
LED	1	1	-	1	-	-
Photoresist	-	-	-	3	-	-
Potentiometer	-	-	-	-	1	1
Piezo	-	-	1	-	-	-
LCD	-	-	-	-	-	1
Battery snap	-	-	-	-	1	-
DC Motor	-	-	-	-	1	-
H-bridge	-	-	-	-	1	-
No. of parts	4	9	17	22	24	23

**Table 4** Assembly complexity of the six assembled electronic boards (P1–P6)

Complexity	P1	P2	P3	P4	P5	P6
$C_1$	1.64	3.12	5.35	6.59	7.49	6.97
$C_2$	2.90	5.89	10.03	13.39	15.83	18.24
$C_3$	0.75	0.57	0.45	0.40	0.37	0.39
$C$	3.80	6.50	9.83	11.95	13.37	14.12

enabling the components to be connected without soldering. Each of the six selected products (P1–P6) required a different number and type of components to connect to the breadboard (see Table 3).

The assembly complexity of the six selected electronic boards was assessed according to the method described in Section. 3.1. Table 4 shows the values calculated for the six selected boards (P1–P6), which were selected to cover a wide range of assembly complexity. Notably, despite the number of parts of product P5 being higher than the number of parts of product P6, the total assembly complexity ( $C$ ) of P6 is higher than that of P5. This is due to the different combinations of complexity components ( $C_1$ ,  $C_2$ ,  $C_3$ ), which consider not only the number of components, but also their nature and connections.

Table 5 reports the handling complexity ( $h_m$ ) and the connection complexity ( $l_{mn}$ ) of each product component of the six electronic boards. Each component has a different value of  $h_m$  and can assume different values of  $l_{mn}$ . Thus, if a product is composed of several components with high handling complexity and high connection complexity, it is more complex to assemble. The different values of  $l_{mn}$  depend on the connection between the parts and the breadboard. For example, the connection complexity of long wires to the breadboard ranges from 3.7 to 6.3, depending on how the component is inserted into the breadboard and on the other components that are already connected. The

**Table 5** Components handling complexity ( $h_m$ ) and connection complexity of each component with the breadboard ( $l_{mn}$ ) in the six electronic board variants (P1–P6)

Component	$h_m$	$l_{mn}$
Breadboard (BB)	1.7	-
Long wires (LW)	1.8	3.7, 5.3, 6.3
Short wires (SW)	2.3	3.7, 5.3
Resistors (R)	1.8	3.8
Pushbuttons (PB)	1.9	4.2
LED (L)	1.9	4.2
Phototransistor (F)	1.9	4.2
Potentiometer (PT)	1.7	5.8
Piezo (PZ)	1.7	3.7
LCD (LCD)	3.0	6.4
Battery snap (BS)	1.8	3.7
DC Motor (M)	1.8	3.7
H-bridge (HB)	1.9	4.2

intermediate connection complexity value of 5.3 is given if the wire needs to be bent to make the connection, while 6.3 is assigned if the connection is made with reduced visibility (as per Table 2). It is important to note that each component is always connected to the breadboard in the specific case of electronic boards (thus,  $n$  is always the breadboard (see Eq. (4) and (6))

In this first experiment, cognitive effort was not taken into account because the aim was to analyse how different assembly configurations of different types of the same product family affected process performance. The aim was therefore to investigate how the complexity of an assembled product (linked to the nature of the product itself) affected the process. Future work plans to integrate cognitive effort of the operator for a broader comparison of different assemblies, using parameters such as electrothermal activity and heart rate variability [29].

## 4 Assembly systems

In order to answer the research questions (*RQ1* and *RQ2*), three different experimental campaigns for the assembly of electronic boards were carried out. The first campaign was a fully manual assembly of the boards, where the operator was responsible for the entire assembly process (see Section. 4.1). In the other two campaigns, a cobot assisted the operator during the entire assembly process, based on their actual application in companies using cobots in assembly. In the first collaborative experiment, the cobot only had logistical functions to pick up the parts at predefined positions (see Section. 4.2), while in the second collaborative experiment, the cobot also recognized the parts to be picked up using a camera (see Section. 4.3). During the experiments, information on assembly times and defects was collected. The aim was to investigate the relationship between time and defects and board assembly complexity, and whether these relationships were affected by the assembly system.

Each of the three experimental campaigns involved six expert operators, different for each experiment, for a total of 18 operators. Before the assembly trials, the operators were given preliminary training to ensure a consistent level of skill among the participants and reduce the impact of varying skill levels on the results. The training aimed to familiarise the operators with the assembly process and equipment. To avoid unwanted learning effects, the six operators assembled the six boards in a random order according to an experimental design.

The assembly process consisted of two distinct phases: an assembly phase and a quality control phase. In the assembly phase, each electronic board was assembled manually or with the cobot support, according to the selected assembly strategy. In this first phase, information on assembly time and in-process defects, i.e. defects occurring during the assembly process [30], was collected. On the other hand, during the quality control phase, an operator experienced in performing quality control checked and detected any remaining defects in the electronic boards. The expert was the same for all three experimental campaigns. During the quality control phase, data on quality control time and offline

defects, i.e. defects detected during the control phase [30], were collected.

The sequence of the assembly operations was the same for all three assembly systems and was predefined according to the circuit theory [31]. In particular, for the circuit to work properly, there should be an uninterrupted path between the power source and the lowest energy point (ground). In addition, the current will always follow the path of least resistance to ground when presented with multiple options since components within the circuit dissipate electrical energy by converting it into different forms, such as light, heat and sound. During the three experimental campaigns, the operators were provided with a PC containing the circuit diagram of the boards to be assembled, in order to facilitate the implementation of the predefined assembly sequence.

### 4.1 Manual assembly system

In the manual assembly experiment, the six operators manually assembled the six electronic boards. The electronic parts were arranged in the ARDUINO UNO starter kit box according to their type (e.g. long wires, short wires, resistors), and the operators searched for and selected the correct part to assemble. Following the predefined assembly strategy, the operators took each part out of the box and assembled it on the breadboard (see Fig. 2a). Thus, in manual assembly, the operator was responsible for all operations, from selecting the parts from the box to the overall assembly. As a result, the operator's cognitive load in manual assembly was significantly higher than in the other two assembly systems. Figure 2b shows the workstation of the manual experiments.

### 4.2 HRC assembly system

In the first collaborative assembly (labelled as HRC assembly), a UR3e cobot by Universal Robots™ was used to assemble the six electronic boards. In the HRC assembly, the human operator was relieved of the task of selecting and picking the correct parts, now done by the cobot. To enable the assembly process, the OnRobot™ RG6 gripper available at Mind4Lab (Manufacturing for Industry 4.0 Laboratory) of Department of Management and Production Engineering of the Politecnico di Torino was used. This type of gripper is often used for handling larger loads. However, its adaptability allows it to be used for handling small components, such as those found in electronic devices. In future applications (see Section. 7), it is planned to use an ad hoc gripper for such electronic components (e.g., the OnRobot™ 2FG7 parallel gripper) in order to reduce the cobot's spatial occupation within the workstation and increase its speed of movement.

Table 6 provides a comprehensive overview of the cobot and gripper parameters used during the collaborative

**Fig. 2** **a** Schematic of the manual assembly process; **b** Manual assembly workstation

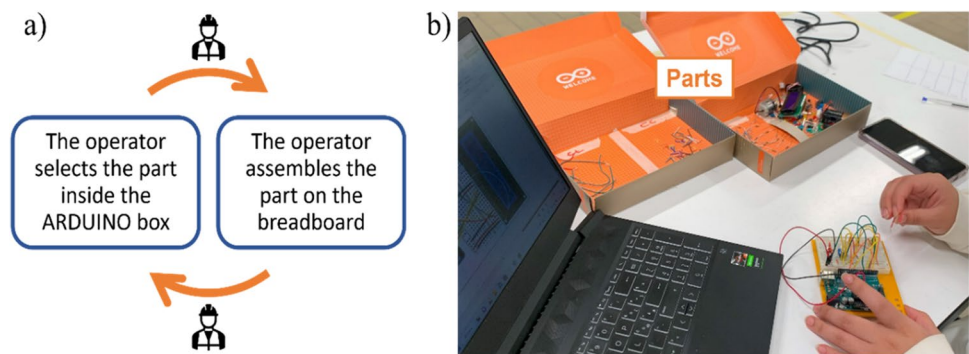


**Table 6** Cobot and gripper parameters

Parameters	Cobot	Gripper
MoveJ speed ( $^{\circ}/s$ )	200	-
MoveJ acc. ( $^{\circ}/s^2$ )	200	-
MoveL speed (mm/s)	200	-
MoveL acc. (mm/s $^2$ )	200	-
Distance (mm)	-	25
Force (N)	-	80

assembly. Specifically, the collaborative robot uses two different types of motions: MoveJ and MoveL. The MoveJ movement involves the simultaneous positioning of each joint, resulting in a curved trajectory for the tool. MoveL, on the other hand, allows the tool to move linearly between waypoints. For both types of motion, the critical parameters for identification are the speed and the maximum acceleration of the joint. For the gripper, the main parameters are the distance between the fingers when the gripper is open and the gripping force when the gripper is closed.

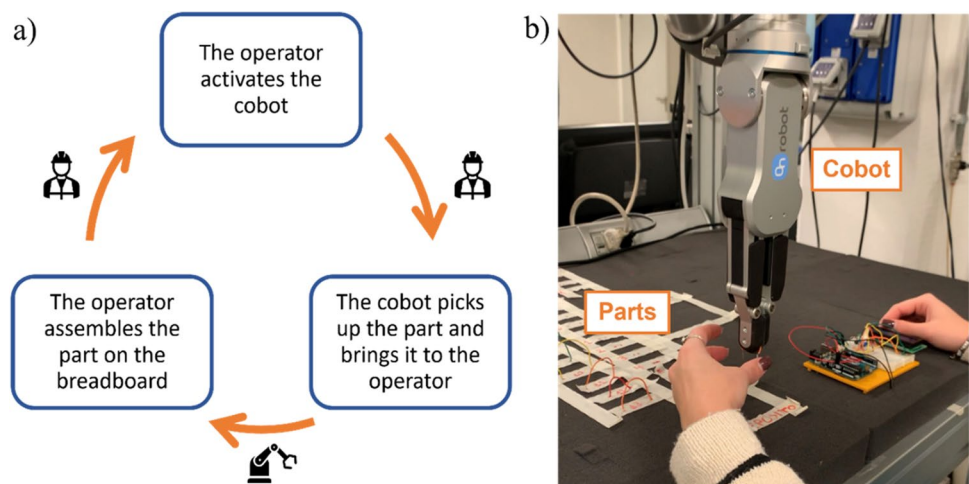
During the assembly phase (see Fig. 3a), the cobot supplied the necessary components to the operator, who assembled the boards in the predetermined order. In particular, the operator controlled the logistics activities by activating

the cobot with a button located near the workstation. Then, the cobot took the parts positioned in a foam support placed on the workstation and handed them to the operator, who connected the supplied part to the breadboard. Obviously, in the absence of a camera, the parts were placed on the foam support in a specific position on the workstation, which was declared to the cobot programming software prior to the experiment. It is important to note that the work-related performance measure is based on assembly time only, which does not include the time spent positioning the parts in the workstation. This exclusion is further supported by the empirical observation that the time required to set up the workstation and arrange the parts in the three assembly systems (manual, HRC, and smart HRC) is comparable (around two minutes for each). Figure 3b shows the collaborative workstation used during the experiment.

### 4.3 Smart HRC assembly system

In the Smart HRC assembly (labelled as S-HRC assembly), the cobot was equipped with the OnRobot™ Eyes camera. OnRobot™ Eyes is an integrated vision system that enables part recognition by the collaborative system. The camera can be positioned on the cobot arm or outside the cobot. However, to accommodate the limited space at the workstation,

**Fig. 3** **a** Schematic of the HRC assembly process; **b** HRC assembly workstation





the camera was positioned outside the cobot (see Fig. 4b). The speeds and movements of the cobot's joints are the same used in the experiment without the camera (see Table 6). However, due to the limited space available in the workstation, the cobot operated at 50% of its maximum speed to avoid accidental collisions between the cobot and the camera. In fact, especially when picking up parts further away from the storage area, the excessive speed of the cobot when returning to the storage area could cause a collision between the joints closer to the base of the cobot and the external camera. The limitations are due to the fact that the workstation, originally designed for different tasks, has been adapted for the current application. Future tests will include a bespoke redesign for the board assembly process and the use of a more specific gripper (see Section. 7).

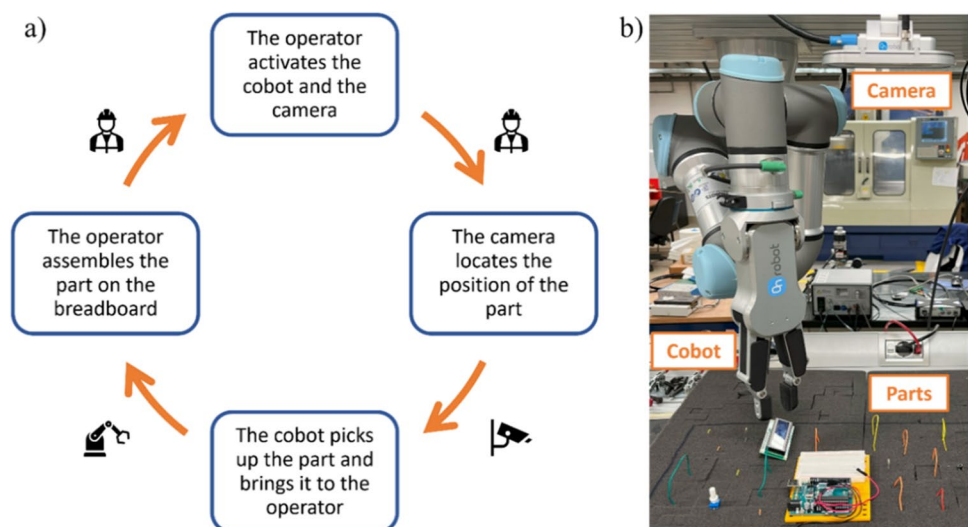
To ensure accurate part recognition, the OnRobot™ Eyes system required an initial camera calibration phase. This involved setting the exposure level, white balance and light intensity emitted by the camera (lighting system allowing the camera to operate independently of the external lighting conditions). For the experiments, the default values specified in the OnRobot™ Eyes manual were used as calibration settings, i.e. exposure level 14%, white balance 20% and light 50%.

After the calibration phase, the camera was programmed to detect the parts using the Eyes Locate function. This function allowed the part detection area to be defined and the detection modes to be selected. Two modes were used in the case study: location by outline and location by colour and size. The location by outline mode was used to detect large components such as the breadboard, LCD, battery snap and DC motor. This mode relied on shape recognition to accurately identify the parts. On the other hand, the location by colour and size mode, which relies on colour and size attributes, was used for all other small components.

Leveraging the capabilities of the OnRobot™ Eyes system, the cobot was able to effectively detect and identify different parts during the assembly process. The combination of external camera placement, camera calibration and the specific detection modes employed facilitated efficient and accurate part recognition, contributing to the overall success of the collaborative assembly task. In addition, this configuration allows the human operator to concentrate more on the assembly operations, freeing him/her from the task of picking up parts. This reduces the cognitive load on the human operator, who tends to make fewer mistakes because fewer tasks have to be performed [32].

As with the HRC assembly, the operator was in control of the process. By pressing a button near the workstation, the operator activated the cobot and the camera for the recognition phase. During this phase, the collaborative system retrieved the components positioned in the foam support placed on the workstation according to the camera's instructions. Using the Eyes Get Workpiece and Eyes Pick functions, the camera communicated the spatial coordinates of the identified workpieces to the cobot. Working at speeds reduced to 50% and according to the parameters shown in Table 6, the cobot picked up the workpieces identified by the camera and transported them to the human operator for assembly. In particular, when faced with two identical parts, the cobot consistently prioritised the selection of the left most part, given its closer proximity to the assembly station. After receiving the part, the operator proceeded to assemble the board following the predefined assembly order. This process, schematized in Fig. 4a, continued until the board assembly was complete. This systematic approach ensures a consistent workflow and facilitates the seamless integration of the cobot's capabilities with the human operator's role in the assembly process.

**Fig. 4** **a** Schematic of the S-HRC assembly process; **b** Smart HRC assembly workstation



## 5 Research method

As mentioned above, data on productivity and quality of the process and product were collected during the three experimental campaigns. The main goal was to investigate the relationship between productivity and quality and the assembly complexity of the six electronic boards. The performance measures for this study were carefully selected considering their alignment with the study objectives and a comprehensive literature review. Although numerous metrics exist for evaluating collaborative systems' performance, the chosen measures of assembly time and total assembly defects were considered the most appropriate for this study due to their widespread use in the manufacturing industry.

Regarding process productivity, information on assembly time and quality control time was collected during each experimental campaign. However, quality control time was not further investigated in each assembly system after testing for non-significance at the 95% confidence level using a one-way ANOVA ( $p$  value greater than the significance level of 0.05). Instead, the assembly time increased more than linearly with the assembly complexity. In particular, according to residual analysis, the most suitable model to represent this relationship was the power law model, as follows:

$$AT = \alpha \cdot C^\beta \quad (8)$$

where  $AT$  is the assembly time,  $C$  is the assembly complexity evaluated according to Eq. (1), and  $\alpha$  and  $\beta$  are the nonlinear regression coefficients. This suggests that the cognitive effort and deliberation time required for assembly operations increases significantly as assembly complexity increases.

Concerning the defects, for each product variant assembled in each assembly system, the total number of defects divided into in-process defects and offline defects was recorded (see Table 7). During the process, the assembly operators and the quality control operator indicate the number of defects found in each category for each assembled board.

A “wrong part” means inserting the wrong part on the board. An example is using a short wire instead of a long wire or using a 10 k $\Omega$  resistor instead of a 1 M $\Omega$  resistor. The “wrong position” defect refers to the incorrect positioning of the component on the breadboard. In this case, the part picked up is correct, but its position on the board is incorrect. “Part not taken” refers to the failure of the cobot to pick up the part required for assembly in collaborative assemblies. A “slipped part” occurs when the cobot picks up the correct part, but it slips during transport to the operator. A “defective part” occurs when the robot or operator damages the part during pick up. Finally, an “incorrectly inserted part” is defined as a correct part that is inserted in the correct position, but not inserted properly to allow current to flow

**Table 7** Classification of in-process and offline defects

Type of defects	Category
Wrong part	Offline
Wrong position	Offline
Part not taken	In-process
Slipped part	In-process
Defective part	Offline
Incorrectly inserted part	Offline

through the circuit. Obviously, Part not taken and Slipped part, which are cobot errors, refer only to the assembly phase of collaborative experiments.

The process defectiveness was analysed in terms of total defects (i.e. the sum of in-process and offline defects), as they are representative of the overall quality of the assembly process. In particular, to study the relationship between total defects and assembly complexity, the Poisson regression model was used, as the total defects are count data [33]. The logarithm and square root link functions were considered, and different models were compared up to the third order of the predictor (i.e. assembly complexity  $C$ ). The selection of the best model was made based on Akaike's corrected information criterion (AICc) and Bayesian information criterion (BIC), goodness-of-fit tests (Deviance and Pearson tests) and deviance residual plots [33, 34]. According to the results, the most appropriate Poisson model was the one using the square root link function, represented as:

$$TD = \gamma \cdot C^2 \quad (9)$$

where  $TD$  is the total number of defects,  $C$  is assembly complexity evaluated according to Eq. (1), and  $\gamma$  is the regression coefficient.

## 6 Results and discussions

### 6.1 Experimental results

According to the models presented in Section. 5, the results of the analysis are reported in Tables 8 and 9. Table 8 refers to productivity data, i.e. assembly time data, whereas Table 9 refers to quality data, i.e. total defects data. For both tables, the data are reported separately for each assembly system (i.e. manual, HRC and S-HRC) and in the order used during the experiments, i.e. a random order (Obs). The experimental values (Value) and the fitted values (Fit) are also provided. The experimental values are those actually collected during the different tests. The fitted values are point estimates of the mean response for given values of the predictors, calculated by entering the

**Table 8** Assembly time (*AT*) results of the three experimental campaigns

Obs	<i>C</i>	Manual			HRC			S-HRC		
		Value	Fit	95% CI	Value	Fit	95% CI	Value	Fit	95% CI
1	11.95	11.42	10.09	(8.97, 11.21)	12.12	10.37	(9.36, 11.38)	8.65	10.30	(9.78, 10.83)
2	14.12	13.50	12.84	(11.16, 14.52)	14.17	13.98	(12.44, 15.52)	16.03	12.99	(12.21, 13.78)
3	3.80	1.38	1.92	(0.66, 3.19)	2.80	1.34	(0.44, 2.24)	1.53	2.10	(1.49, 2.72)
4	13.37	9.92	11.87	(10.48, 13.26)	11.13	12.68	(11.45, 13.90)	11.07	12.04	(11.39, 12.69)
5	9.83	9.83	7.61	(6.34, 8.88)	6.57	7.31	(6.09, 8.54)	7.85	7.86	(7.27, 8.44)
6	6.50	3.35	4.18	(2.64, 5.73)	2.97	3.50	(2.17, 4.83)	3.73	4.43	(3.71, 5.16)
7	13.37	9.98	11.87	(10.48, 13.26)	13.10	12.68	(11.45, 13.90)	9.50	12.04	(11.39, 12.69)
8	11.95	10.02	10.09	(8.97, 11.21)	9.00	10.37	(9.36, 11.38)	7.75	10.30	(9.78, 10.83)
9	9.83	4.68	7.61	(6.34, 8.88)	6.50	7.31	(6.09, 8.54)	8.58	7.86	(7.27, 8.44)
10	14.12	8.95	12.84	(11.16, 14.52)	14.25	13.98	(12.44, 15.52)	11.70	12.99	(12.21, 13.78)
11	6.50	2.60	4.18	(2.64, 5.73)	3.30	3.50	(2.17, 4.83)	3.73	4.43	(3.71, 5.16)
12	3.80	0.95	1.92	(0.66, 3.19)	1.32	1.34	(0.44, 2.24)	1.58	2.10	(1.49, 2.72)
13	9.83	12.62	7.61	(6.33, 8.88)	10.20	7.31	(6.09, 8.54)	8.65	7.86	(7.27, 8.44)
14	14.12	19.58	12.84	(11.16, 14.52)	17.48	13.98	(12.44, 15.52)	13.50	12.99	(12.21, 13.78)
15	3.80	2.08	1.92	(0.66, 3.19)	1.37	1.34	(0.44, 2.24)	1.65	2.10	(1.49, 2.72)
16	11.95	9.33	10.09	(8.97, 11.21)	10.03	10.37	(9.36, 11.38)	8.75	10.30	(9.78, 10.83)
17	6.50	4.22	4.18	(2.64, 5.73)	4.98	3.50	(2.17, 4.83)	5.88	4.43	(3.71, 5.16)
18	13.37	11.48	11.87	(10.48, 13.26)	13.15	12.68	(11.45, 13.90)	10.93	12.04	(11.39, 12.69)
19	6.50	6.40	4.18	(2.64, 5.73)	3.37	3.50	(2.17, 4.83)	4.48	4.43	(3.71, 5.16)
20	11.95	10.32	10.09	(8.97, 11.21)	8.85	10.37	(9.36, 11.38)	9.23	10.30	(9.78, 10.83)
21	3.80	2.42	1.92	(0.66, 3.19)	1.57	1.34	(0.44, 2.24)	1.98	2.10	(1.49, 2.72)
22	9.83	5.92	7.61	(6.34, 8.88)	6.57	7.31	(6.09, 8.54)	8.87	7.86	(7.27, 8.44)
23	14.12	11.95	12.84	(11.16, 14.52)	11.83	13.99	(12.44, 15.52)	16.02	12.99	(12.21, 13.78)
24	13.37	9.45	11.87	(10.48, 13.26)	9.28	12.68	(11.45, 13.90)	12.23	12.04	(11.39, 12.69)
25	3.80	1.47	1.92	(0.66, 3.19)	1.75	1.34	(0.44, 2.24)	1.88	2.10	(1.49, 2.72)
26	9.83	5.43	7.61	(6.34, 8.88)	5.83	7.31	(6.09, 8.54)	9.98	7.86	(7.27, 8.44)
27	13.37	7.43	11.87	(10.48, 13.26)	8.85	12.68	(11.45, 13.90)	14.70	12.04	(11.39, 12.69)
28	14.12	9.53	12.84	(11.16, 14.52)	10.43	13.98	(12.44, 15.52)	12.18	12.99	(12.21, 13.78)
29	11.95	7.23	10.09	(8.97, 11.21)	5.78	10.37	(9.36, 11.38)	11.23	10.30	(9.78, 10.83)
30	6.50	4.22	4.18	(2.64, 5.73)	1.98	3.50	(2.17, 4.83)	5.03	4.43	(3.71, 5.16)
31	14.12	22.77	12.84	(11.16, 14.52)	23.73	13.98	(12.44, 15.52)	12.00	12.99	(12.21, 13.78)
32	6.50	5.17	4.18	(2.64, 5.73)	6.97	3.50	(2.17, 4.83)	4.40	4.43	(3.71, 5.16)
33	13.37	10.53	11.87	(10.48, 13.26)	14.80	12.68	(11.45, 13.90)	12.00	12.04	(11.39, 12.69)
34	9.83	9.08	7.61	(6.34, 8.88)	8.22	7.31	(6.09, 8.54)	8.60	7.86	(7.27, 8.44)
35	3.80	2.42	1.92	(0.66, 3.19)	2.53	1.34	(0.44, 2.24)	2.02	2.10	(1.49, 2.72)
36	11.95	13.40	10.09	(8.97, 11.21)	11.35	10.37	(9.36, 11.38)	9.97	10.30	(9.78, 10.83)

specific values for each observation in the data set into the regression model equation. The fitted values in Table 8 were obtained according to Eq. (8), while the fitted values in Table 9 were obtained according to Eq. (9). For each fitted value, the corresponding 95% confidence intervals are reported. The regression coefficients with their 95% CIs are reported in Table 10 (see Section. 6.2).

According to the model in Eqs. (8) and (9) and the data in Tables 8 and 9, research question *RQ1* (reported in Section. 1) can be answered with the following finding:

- *FI*: The assembly complexity and the characteristics of a product within a product family affect the productivity and the quality of assembly processes.

This finding is valid for all three assembly systems, both in terms of assembly times and total defects. In fact, according to Eq. (8), assembly times (associated to process productivity) increase following a power trend when increasing assembly complexity. This implies that an increase in assembly complexity leads to a more than proportional increase

**Table 9** Total defects (*TD*) results of the three experimental campaigns

Obs	<i>C</i>	Manual			HRC			S-HRC		
		Value	Fit	95% CI	Value	Fit	95% CI	Value	Fit	95% CI
1	11.95	6	4.45	(3.71, 5.26)	3	2.96	(2.36, 3.63)	5	8.18	(7.17, 9.27)
2	14.12	6	6.21	(5.17, 7.34)	7	4.14	(3.30, 5.07)	15	11.44	(10.01, 12.96)
3	3.80	2	0.45	(0.38, 0.53)	0	0.30	(0.24, 0.37)	0	0.83	(0.73, 0.94)
4	13.37	5	5.57	(4.64, 6.58)	5	3.71	(2.96, 4.55)	6	10.25	(8.95, 11.61)
5	9.83	9	3.01	(2.51, 3.56)	3	2.01	(1.60, 2.46)	0	5.54	(4.85, 6.28)
6	6.50	3	1.32	(1.10, 1.56)	1	0.88	(0.70, 1.08)	1	2.43	(2.12, 2.75)
7	13.37	3	5.57	(4.64, 6.58)	4	3.71	(2.96, 4.55)	10	10.25	(8.97, 11.61)
8	11.95	4	4.45	(3.71, 5.26)	3	2.96	(2.36, 3.63)	7	8.18	(7.17, 9.27)
9	9.83	0	3.01	(2.51, 3.56)	3	2.01	(1.60, 2.46)	7	5.54	(4.85, 6.28)
10	14.12	5	6.21	(5.17, 7.34)	5	4.14	(3.30, 5.07)	15	11.44	(10.01, 12.97)
11	6.50	1	1.32	(1.10, 1.56)	0	0.88	(0.70, 1.08)	1	2.43	(2.12, 2.75)
12	3.80	0	0.45	(0.38, 0.53)	0	0.30	(0.24, 0.37)	2	0.83	(0.73, 0.94)
13	9.83	2	3.01	(2.51, 3.56)	0	2.01	(1.60, 2.46)	9	5.54	(4.85, 6.28)
14	14.12	4	6.21	(5.17, 7.34)	6	4.14	(3.30, 5.07)	12	11.44	(10.01, 12.96)
15	3.80	0	0.45	(0.38, 0.53)	0	0.30	(0.24, 0.37)	0	0.83	(0.73, 0.94)
16	11.95	0	4.45	(3.71, 5.26)	3	2.96	(2.36, 3.63)	6	8.18	(7.17, 9.27)
17	6.50	0	1.32	(1.10, 1.56)	2	0.88	(0.70, 1.08)	3	2.43	(2.12, 2.75)
18	13.37	0	5.57	(4.64, 6.58)	3	3.71	(2.96, 4.55)	13	10.25	(8.97, 11.61)
19	6.50	0	1.32	(1.10, 1.56)	2	0.88	(0.70, 1.08)	8	2.43	(2.12, 2.75)
20	11.95	2	4.45	(3.71, 5.26)	3	2.96	(2.36, 3.63)	6	8.18	(7.17, 9.27)
21	3.80	0	0.45	(0.38, 0.53)	0	0.30	(0.24, 0.37)	2	0.83	(0.72, 0.94)
22	9.83	1	3.01	(2.51, 3.56)	0	2.00	(1.60, 2.46)	8	5.54	(4.85, 6.28)
23	14.12	11	6.21	(5.17, 7.34)	4	4.14	(3.30, 5.07)	12	11.44	(10.01, 12.96)
24	13.37	3	5.57	(4.64, 6.58)	6	3.71	(2.96, 4.55)	11	10.25	(8.97, 11.61)
25	3.80	0	0.45	(0.38, 0.53)	0	0.30	(0.24, 0.37)	0	0.83	(0.73, 0.94)
26	9.83	4	3.01	(2.51, 3.56)	2	2.00	(1.60, 2.46)	5	5.54	(4.85, 6.28)
27	13.37	5	5.57	(4.64, 6.58)	3	3.71	(2.96, 4.55)	20	10.25	(8.98, 11.61)
28	14.12	9	6.21	(5.17, 7.34)	5	4.14	(3.30, 5.07)	12	11.44	(10.01, 12.96)
29	11.95	11	4.45	(3.71, 5.26)	0	2.96	(2.36, 3.63)	4	8.18	(7.17, 9.27)
30	6.50	0	1.32	(1.10, 1.56)	1	0.88	(0.70, 1.08)	3	2.43	(2.12, 2.75)
31	14.12	13	6.21	(5.17, 7.34)	6	4.14	(3.30, 5.07)	7	11.44	(10.01, 12.96)
32	6.50	0	1.32	(1.10, 1.56)	0	0.88	(0.70, 1.08)	4	2.43	(2.12, 2.75)
33	13.37	8	5.57	(4.64, 6.58)	1	3.71	(2.96, 4.55)	6	10.25	(8.97, 11.61)
34	9.83	2	3.01	(2.51, 3.56)	1	2.00	(1.60, 2.46)	6	5.54	(4.85, 6.28)
35	3.80	0	0.45	(0.38, 0.53)	0	0.30	(0.24, 0.37)	0	0.83	(0.73, 0.94)
36	11.95	7	4.45	(3.71, 5.26)	2	2.96	(2.36, 3.63)	6	8.18	(7.17, 9.27)

**Table 10** Main outputs from non-linear regression for assembly time vs assembly complexity and Poisson regression for total defects vs assembly complexity

System	$\alpha$	SE( $\alpha$ )	$\beta$	SE( $\beta$ )	$\gamma$	SE( $\gamma$ )	95% CI ( $\alpha$ )	95% CI ( $\beta$ )	95% CI ( $\gamma$ )
Manual	0.28	0.19	1.45	0.27	0.18	0.01	(0.05, 0.92)	(0.97, 2.11)	(0.16, 0.19)
HRC	0.12	0.09	1.79	0.27	0.14	0.01	(0.02, 0.45)	(1.28, 2.49)	(0.13, 0.15)
S-HRC	0.33	0.10	1.39	0.12	0.24	0.01	(0.17, 0.58)	(1.16, 1.65)	(0.22, 0.26)

in assembly time. On the other hand, according to Eq. (9), the relationship between defects (associated to process quality) and assembly complexity is modelled using a Poisson

model with square root link function. Thus, also total defects increase more than linearly with increasing assembly complexity. These results show that increased assembly



complexity leads to more defects, not just because of the higher number of components, but due to the intricate interactions and precision required for connections. Each additional element introduces new potential for errors, extending assembly time and raising the defect rate. This finding aligns with previous studies in this domain, which was primarily conducted on distinct electromechanical products and workstations without a specific emphasis on product families [19, 28]. Therefore, the uniqueness of the current study lies in its examination and quantification of assembly complexity's influence on productivity and quality within the context of a product family, encompassing a range of products with varying degrees of complexity in different assembly processes.

## 6.2 Comparison between assembly systems

In order to answer the second research question (*RQ2*), the curves in Fig. 5 were plotted using the data from Tables 8 and 9. Figure 5 shows the regression curves of assembly time (Fig. 5a) and total defects (Fig. 5b) versus assembly complexity for the three assembly systems. Each curve is presented with its respective 95% confidence intervals, indicating that the regression lines closely follow the curvature of the points and that there are no systematic deviations from the fitted lines. It has to be noted that in Fig. 5, the 95% confidence intervals are limited to zero (for both assembly times and total defects) since time and defects cannot assume negative values.

Regarding assembly time, as mentioned in Section. 5, it increases more than linearly with assembly complexity for all three systems. This trend is modelled by the power law model defined in Eq. (8). Figure 5a shows the three curves, one for each system, which describe this relationship between assembly time and assembly complexity. Since the 95% confidence intervals of the three regression curves overlap, no statistical differences between the three assembly systems in terms of assembly times at the 5% significance level are evidenced.

On the other hand, as far as total defects are concerned (see Fig. 5b), in all three assembly systems, the total assembly defects follow the same trend as a function of assembly

complexity, i.e. the Poisson model with a square root link function, according to Eq. (8). As shown in Fig. 5b, the 95% confidence intervals of the three regression curves do not overlap. This implies that there is a difference in the estimated ranges of total defects produced by each of the three assembly systems (i.e. significant differences between manual and HRC, manual and S-HRC, HRC and S-HRC scenarios). Consequently, the lack of overlap between these intervals for the three systems indicates that the differences in mean total defects between the systems are statistically significant at the 5% significance level.

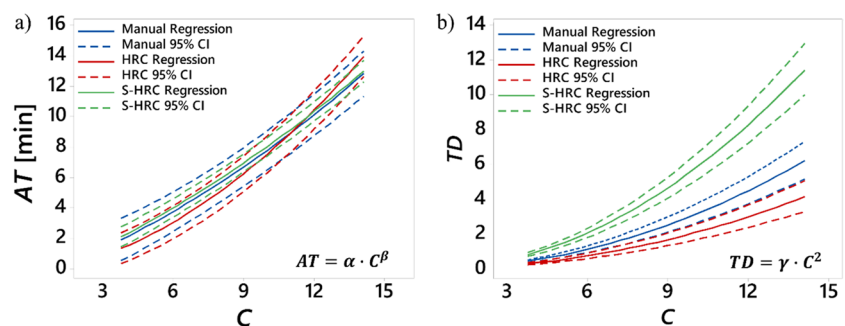
The same considerations can be inferred from a numerical point of view by analysing the data in Table 10, which presents the main results of the regression curves shown in Fig. 5. Table 10 reports the estimated regression parameters ( $\alpha$ ,  $\beta$ ,  $\gamma$ ), their standard error ( $SE(\alpha)$ ,  $SE(\beta)$  and  $SE(\gamma)$ ), i.e. the variation in the estimated mean response for the predictors, and the 95% confidence interval for each regression parameter. In particular, regarding assembly time, Table 10 shows that the 95% confidence intervals for the  $\alpha$  and  $\beta$  parameters of all three assembly systems models overlap. On the other hand, in terms of total defects, Table 10 shows that the three 95% confidence intervals of  $\gamma$  do not overlap.

Thus, in responding to the second research question *RQ2* (reported in Section. 1), the following finding is obtained:

- *F2*: A statistically significant difference exists in the quality of the assembly process across various assembly systems when applied to different products within a product family. Conversely, such a difference is not observed in the productivity of the assembly process.

This new finding, which has not been analysed in previous studies, is quite interesting. In fact, the results show that the way in which parts are selected and transported by or to the operator, whether in manual or cobot-assisted systems, does not significantly affect assembly times. As a result, the analysis shows that there are no significant differences in the assembly times associated with the manual, HRC and S-HRC systems at the 5% significance level. This result is particularly noteworthy given that the S-HRC

**Fig. 5** Comparison between Manual, HRC and S-HRC systems on (a) assembly time (*AT*) and (b) total defects (*TD*)



system operates the cobot at a reduced speed of 50%. This underlines the promising potential of this intelligent system; optimal usage could potentially translate to a substantial reduction in assembly time. In the context of this case study, however, fully realising this potential would necessitate alterations to the collaborative system's workstation architecture or the adoption of a more refined camera for part recognition.

On the other hand, in terms of quality, the assembly system influences the occurrence of total assembly defects. On closer inspection, and using a 5% significance level, the results show that the HRC system generates fewer errors than the manual system, which in turn produces fewer errors than the S-HRC system. Accordingly, in this specific case study, the HRC system outperforms in terms of quality as it effectively eliminates part selection errors, a common issue in manual assembly. Barring situations where the part is incorrectly picked or slips during transport to the operator, the cobot consistently delivers accurate selection. Contrary to expectations, the S-HRC assembly system exhibited the highest total defects. The primary factor contributing to this outcome is the restricted and the instability of the current camera vision system, which has proved inadequate in consistently and accurately recognizing the parts to be assembled. It is important to note that the parts comprising the breadboard are quite small, with diverse colours and sizes, which can exacerbate the challenge. The camera currently in use is low resolution and, coupled with the still-maturing system, leads to a high error rate in part recognition. The characteristics of the assembled parts—their minute size, different colours and sizes—present an intricate scenario for the vision system, causing it to struggle with part recognition accuracy. However, these findings should not be misinterpreted as inherent flaws within the S-HRC assembly system itself. Instead, they underscore the urgent need to enhance the vision system, particularly its ability to accurately recognise a range of distinct parts. This could be achieved either by using a higher resolution camera or by refining the image processing algorithms. These improvements could ultimately optimise both the productivity and quality of the S-HRC assembly system.

## 7 Conclusions

In recent decades, collaborative robots have gained popularity in assembly processes due to their ability to work alongside human workers, improving efficiency and safety. This study has explored the effect of assembly complexity on assembly time and total defects across three distinct assembly systems, specifically designed for electronic board assemblies within a product family. The Manual system involved full manual assembly of the boards, while the

human–robot collaboration (HRC) system utilised a cobot for the pick-and-place tasks. The Smart Human–Robot Collaboration (S-HRC) system expanded upon the HRC setup by incorporating a camera for part recognition. The aim is to address a range of issues related to modern manufacturing, such as the benefits of human–robot collaboration, the difficulties of system integration and the impact of such integration on output and assembly quality.

Across all three experimental settings, a power-law trend was observed linking increased assembly complexity with extended assembly time. Interestingly, no significant difference in assembly time was found between the three systems at the 95% confidence level. When focusing on total defects, a super-linear increase with increasing assembly complexity was also observed. However, the three systems exhibited notable differences. Specifically, the HRC system outperformed, showing the highest quality output, followed by the manual system. The S-HRC system lagged behind, with a significantly higher total number of defects compared to the other two systems. The main factors contributing to this discrepancy were the inadequate camera capability for accurate part recognition within the S-HRC system and the limited space within the workstation.

Addressing the research questions posed, the study findings confirmed that assembly complexity plays a significant role in influencing both assembly time and total assembly defects (*RQ1*). Furthermore, the use of different assembly systems leads to significant differences (at the 5% significance level) only for total assembly defects, but not for assembly time (*RQ2*). It is important to note that these results are based on experiments with certain initial constraints. Hence, future research plans to venture into other facets of Human–Robot Collaboration, which includes cobot engagement in more complex tasks, with human intervention directed towards support and critical decision-making. The use of machine learning algorithms to define real-time strategies (instead of pre-set ones) based on the parts available at the workstation is another future research prospect.

In conclusion, the S-HRC, despite its current limitations, shows promise as a solution to the assembly process within product families, particularly for components with a high number of customizable variants. Its vision system reduces the necessity for frequent workstation reconfiguration and lessens the time and effort spent on part selection compared to both the HRC and Manual systems. Even with a limited operating speed due to space limitations, the S-HRC system still yields assembly times statistically comparable to the other systems. However, the underdeveloped camera vision system, particularly its struggle to accurately recognize smaller parts such as cables, led to a higher defect rate.

Future research will prioritise the refinement of the vision system and the expansion of sample sizes to increase statistical robustness and improve the generalisability of

findings. At the same time, the quantification of cognitive effort expended by operators during various assembly tasks will be explored to provide a more nuanced understanding of assembly complexity. In addition, a critical objective on the horizon involves the development of bespoke workstations and gripping mechanisms tailored for electronic board assembly. This initiative is driven by the need to overcome existing spatial constraints and to optimise the assembly environment. By integrating customised physical interfaces, this strategy aims to streamline assembly operations, potentially reducing assembly times and defect generation. This multi-faceted approach, which blends technological upgrades with ergonomic innovations, will strengthen the overall effectiveness of the S-HRC system in the context of electronic board assembly, providing a comprehensive strategy for enhancing both human and system performance.

**Author contribution** All authors contributed to the study conception and design. Experimental tests, material preparation and data collection were performed by Stefano Puttero. Data analyses were performed by Stefano Puttero and Elisa Verna. The first draft of the manuscript was written by Stefano Puttero, and all authors commented on previous versions of the manuscript. All authors read and approved the final manuscript.

**Funding** Open access funding provided by Politecnico di Torino within the CRUI-CARE Agreement.

## Declarations

**Competing interests** The authors declare no competing interests.

**Open Access** This article is licensed under a Creative Commons Attribution 4.0 International License, which permits use, sharing, adaptation, distribution and reproduction in any medium or format, as long as you give appropriate credit to the original author(s) and the source, provide a link to the Creative Commons licence, and indicate if changes were made. The images or other third party material in this article are included in the article's Creative Commons licence, unless indicated otherwise in a credit line to the material. If material is not included in the article's Creative Commons licence and your intended use is not permitted by statutory regulation or exceeds the permitted use, you will need to obtain permission directly from the copyright holder. To view a copy of this licence, visit <http://creativecommons.org/licenses/by/4.0/>.

## References

- Berx N, Decré W, Morag I et al (2022) Identification and classification of risk factors for human-robot collaboration from a system-wide perspective. *Comput Ind Eng* 163:107827. <https://doi.org/10.1016/j.cie.2021.107827>
- Peshkin M, Colgate JE (1999) Cobots *Ind Robot An Int J* 26:335–341. <https://doi.org/10.1108/01439919910283722>
- Hentout A, Aouache M, Maoudj A, Akli I (2019) Human–robot interaction in industrial collaborative robotics: a literature review of the decade 2008–2017. *Adv Robot* 33:764–799
- Yonga Chuengwa T, Swanepoel JA, Kurien AM et al (2023) Research perspectives in collaborative assembly: a review. *Robotics* 12:37. <https://doi.org/10.3390/robotics12020037>
- Lasi H, Fettek P, Kemper H-G et al (2014) Industry 4.0. *Bus Inf Syst Eng* 6:239–242
- Falck A-C, Örtengren R, Rosenqvist M, Söderberg R (2017) Basic complexity criteria and their impact on manual assembly quality in actual production. *Int J Ind Ergon* 58:117–128. <https://doi.org/10.1016/j.ergon.2016.12.001>
- Lim KYH, Zheng P, Chen CH, Huang L (2020) A digital twin-enhanced system for engineering product family design and optimization. *J Manuf Syst* 57:82–93. <https://doi.org/10.1016/J.JMSY.2020.08.011>
- Barravecchia F, Bartolomei M, Mastrogiacomo L, Franceschini F (2023) Redefining human–robot symbiosis: a bio-inspired approach to collaborative assembly. *Int J Adv Manuf Technol* 128:2043–2058. <https://doi.org/10.1007/s00170-023-11920-1>
- Statista (2022) Collaborative robots worldwide. <https://www.statista.com/topics/8062/collaborative-robots-worldwide/#topicOverview>. Accessed 30 Jun 2023
- Verna E, Genta G, Galetto M (2023) A new approach for evaluating experienced assembly complexity based on Multi Expert-Multi Criteria Decision Making method. *Res Eng Des* 34:301–325. <https://doi.org/10.1007/s00163-023-00409-3>
- Huang J, Pham DT, Li R et al (2021) An experimental human-robot collaborative disassembly cell. *Comput Ind Eng* 155:107189. <https://doi.org/10.1016/j.cie.2021.107189>
- Bilberg A, Malik AA (2019) Digital twin driven human–robot collaborative assembly. *CIRP Ann* 68:499–502. <https://doi.org/10.1016/J.CIRP.2019.04.011>
- Malik AA, Bilberg A (2019) Complexity-based task allocation in human-robot collaborative assembly. *Ind Robot Int J Robot Res Appl* 46:471–480. <https://doi.org/10.1108/IR-11-2018-0231>
- Wang L, Gao R, Váncza J et al (2019) Symbiotic human-robot collaborative assembly. *CIRP Ann* 68:701–726. <https://doi.org/10.1016/j.cirp.2019.05.002>
- Pichler A, Akkaladevi SC, Ikeda M et al (2017) Towards shared autonomy for robotic tasks in manufacturing. In: 27th International Conference on Flexible Automation and Intelligent Manufacturing, FAIM2017. Procedia Manufacturing, 27–30 June 2017, Modena, Italy, 72–82
- Andronas D, Kampourakis E, Papadopoulos G et al (2023) Towards seamless collaboration of humans and high-payload robots: an automotive case study. *Robot Comput Integr Manuf* 83:102544. <https://doi.org/10.1016/J.RCIM.2023.102544>
- D'Souza F, Costa J, Pires JN (2020) Development of a solution for adding a collaborative robot to an industrial AGV. *Ind Robot Int J Robot Res Appl* 47:723–735. <https://doi.org/10.1108/IR-01-2020-0004>
- Falck AC, Rosenqvist M (2012) What are the obstacles and needs of proactive ergonomics measures at early product development stages? – an interview study in five Swedish companies. *Int J Ind Ergon* 42:406–415. <https://doi.org/10.1016/J.ERGON.2012.05.002>
- Alkan B, Vera DA, Ahmad M et al (2018) Complexity in manufacturing systems and its measures: a literature review. *Eur J Ind Eng* 12:116–150
- Lv Q, Zhang R, Liu T et al (2022) A strategy transfer approach for intelligent human-robot collaborative assembly. *Comput Ind Eng* 168:108047. <https://doi.org/10.1016/j.cie.2022.108047>
- Alkan B, Vera D, Ahmad B, Harrison R (2017) A method to assess assembly complexity of industrial products in early design phase. *IEEE Access* 6:989–999
- Sinha K, Suh ES, de Weck O (2018) Integrative complexity: an alternative measure for system modularity. *J Mech Des* 140. <https://doi.org/10.1115/1.4039119>

23. ElMaraghy W, ElMaraghy H, Tomiyama T, Monostori L (2012) Complexity in engineering design and manufacturing. *CIRP Ann* 61:793–814
24. Liu P, Li Z (2012) Task complexity: a review and conceptualization framework. *Int J Ind Ergon* 42:553–568
25. Capponi M, Mastrogiacomio L, Franceschini F (2023) General remarks on the entropy-inspired MCAT (manufacturing complexity assessment tool) model to assess product assembly complexity. *Prod Eng*. <https://doi.org/10.1007/s11740-023-01212-8>
26. Hückel E (1932) Quantentheoretische Beiträge zum Problem der aromatischen und ungesättigten Verbindungen. III *Zeitschrift für Phys* 76:628–648
27. Chan V, Salustri FA (2003) Dfa: The Lucas method. Ryerson University, Toronto
28. Verna E, Genta G, Galetto M, Franceschini F (2022) Defect prediction for assembled products: a novel model based on the structural complexity paradigm. *Int J Adv Manuf Technol* 120:3405–3426
29. Verna E, Puttero S, Genta G, Galetto M (2023) A novel diagnostic tool for human-centric quality monitoring in human–robot collaboration manufacturing. *J Manuf Sci Eng* 145. <https://doi.org/10.1115/1.4063284>
30. Franceschini F, Galetto M, Genta G, Maisano DA (2018) Selection of quality-inspection procedures for short-run productions. *Int J Adv Manuf Technol* 99:2537–2547. <https://doi.org/10.1007/s00170-018-2648-8>
31. Zadeh L (1962) From circuit theory to system theory. *Proc IRE* 50:856–865. <https://doi.org/10.1109/JRPROC.1962.288302>
32. Verna E, Puttero S, Genta G, Galetto M (2023) Exploring the effects of perceived complexity criteria on performance measures of human–robot collaborative assembly. *J Manuf Sci Eng* 145:101014. <https://doi.org/10.1115/1.4063232>
33. Cameron AC, Trivedi PK (2013) Regression analysis of count data. Cambridge University Press
34. Myers RH, Montgomery DC, Vining GG, Robinson TJ (2012) Generalized linear models: with applications in engineering and the sciences. John Wiley & Sons, Hoboken, NJ, USA

**Publisher's Note** Springer Nature remains neutral with regard to jurisdictional claims in published maps and institutional affiliations.